34th Annual International Conference of the IEEE EMBS
San Diego, California USA, 28 August - 1 September, 2012

Towards a Predictive Model of Electroporation-Based Therapies using Pre-Pulse Electrical Measurements

Paulo A. Garcia, *IEEE Member,* Christopher B. Arena, *IEEE Member,* and

Rafael V. Davalos, *IEEE Member*

Invited Paper

***Abstract*— Electroporation-based therapies have been gaining momentum as minimally invasive techniques to facilitate transport of exogenous agents, or directly kill tumors and other undesirable tissue in a non-thermal manner. Typical procedures involve placing electrodes into or around the treatment area and delivering a series of short and intense electric pulses to the tissue/tumor. These pulses create defects in the cell membranes, inducing non-linear changes in the electric conductivity of the tissue. These dynamic conductivity changes redistribute the electric field, and thus the treatment volume. In this study, we develop a statistical model that can be used to determine the baseline conductivity of tissues prior to electroporation and is capable of predicting the non-linear current response with implications for treatment planning and outcome confirmation.**

I. INTRODUCTION

Electroporation-based therapies (EBTs) are clinical procedures that utilize pulsed electric fields to induce nanoscale defects in cell membranes. Typically, pulses are applied through minimally invasive needle electrodes inserted directly into the target tissue, and the pulse parameters are tuned to create either reversible or irreversible defects. Reversible electroporation facilitates the transport of molecules into cells without directly compromising cell viability. This has shown great promise for treating cancer when used in combination with chemotherapeutic agents [1] or plasmid DNA [2]. Alternatively, irreversible electroporation (IRE) has been recognized as a non-thermal tissue ablation modality [3] that produces a tissue lesion, which is visible in real-time on multiple imaging platforms [4, 5]. Because the mechanism of cell death does not rely on thermal processes, IRE spares major nerve and blood vessel architecture [6] and is not subjected to local heat sink effects. These unique benefits have translated to the successful treatment of several surgically "inoperable" tumors [7-9].

In EBTs, the electric field distribution is the primary factor for dictating defect formation and the resulting volume of treated tissue [10, 11]. The electric field is influenced by both the geometry and positioning of the electrodes as well as the dielectric tissue properties. Because the pulse duration (~100 μs) is much longer than the pulse rise/fall time (~100 ns), static solutions of the Continuity equation incorporating only electric conductivity are sufficient for predicting the electric field distribution. In tissues with uniform conductivity, solutions can be obtained analytically for various needle electrode configurations if the exposure length is much larger than the separation distance [12]. This is not often the case in clinical applications where aberrant masses with a diameter on the order of 1 cm are treated with an electrode exposure length of similar dimensions. Additionally, altered membrane permeability due to electroporation influences the tissue conductivity in a non-linear manner. Therefore numerical techniques are required to account for any electrode configuration and incorporate a tissue-specific function relating the electrical conductivity to the electric field distribution (i.e. extent of electroporation).

Recent developments in detecting, monitoring, and imaging electroporation involve complex control algorithms to achieve safe and effective electrogenetherapy and electrical impedance tomography to generate images of the treated regions [4, 13]. Although these methods are promising, they require the delivery of the electroporation pulses to trigger the control algorithms and/or generate the images of the treated regions in a retrospective manner. In addition, they may require additional electronics and the placement of external electrode arrays for analysis. Here we provide an algorithm that can be implemented into pulse generators before the delivery of electroporation-based treatments. The best-fit statistical model uses a pre-pulse to determine the baseline tissue conductivity prior to electroporation, allowing physicians to be actively engaged in treatment planning that accounts for tissue-to-tissue and patient-to-patient variability. By monitoring current through the electrodes placed for treatment, it is possible to predict the extent of electroporation in the tissue and accurately provide physicians with real-time IRE treatment volumes before pulse delivery. The predictions require prior knowledge of the tissue-specific conductivity function and electric field threshold for either reversible electroporation or cell death in the case of IRE. Our group has characterized this non-linear conductivity behavior in *ex vivo* porcine kidney tissue [14]. Using this information, a comprehensive

Manuscript received March 29, 2012. This work was supported by the Coulter Foundation, the NSF under Awards CBET-0933335 and CAREER CBET-1055913, and ICTAS Multi-scale Bio-Engineered Devices and Systems (MBEDS) Center at Virginia Tech.

R.V. Davalos, Ph.D., C.B. Arena, and P.A. Garcia, Ph.D., are with the Virginia Tech-Wake Forest University School of Biomedical Engineering and Sciences, Blacksburg, VA 24061 USA (phone:540-231-1979, email: davalos@vt.edu; carena@vt.edu; pgarcia@vt.edu).

parametric study was performed on electrode exposure length, electrode spacing, voltage-to-distance ratio, and ratio between the maximum conductivity post-IRE and baseline conductivity pre-IRE. Current measurements from all 1440 possible parameter combinations were fit to a statistical model accounting for interaction. The resulting equation is capable of relating pre- and post-IRE current measurements to extrapolate changes in the electric field distribution for any treatment protocol.

II. Materials And Methods

The tissue was modeled as a 10-cm diameter spherical domain using a finite element package (Comsol 4.2a, Stockholm, Sweden). Electrodes were modeled as two 1.0-mm diameter blunt tip needles with exposure lengths (*Y*) and edge-to-edge separation distances (*X*) given in Table 1. The electrode domains were subtracted from the tissue domain, effectively modeling the electrodes as boundary conditions.

The electric field distribution associated with the applied pulse is given by solving the Continuity equation:

$$\nabla \cdot \left(\sigma\left(|E|\right)\nabla \varphi\right) = 0 \qquad (1)$$

where σ is the electrical conductivity of the tissue, *E* is the electric field in V/cm, and φ is the electrical potential [10]. Boundaries along the tissue in contact with the energized electrode were defined as $\varphi = V_o$, and boundaries at the interface of the other electrode were set to ground. The applied voltages were manipulated to ensure that the voltage-to-distance ratios (*W*) corresponded to those in Table 1. The remaining boundaries were treated as electrically insulating, $\partial\varphi/\partial n = 0$.

The analyzed domain extends far enough from the area of interest (i.e. the area near the electrodes) that the electrically insulating boundaries at the edges of the domain do not significantly influence the results in the treatment zone. We used the physics-controlled finer mesh with ~100,000 elements. The numerical models were adapted to account for a dynamic tissue conductivity that occurs as a result of electroporation, which is described by an asymmetrical Gompertz curve for renal porcine tissue [14]:

$$\sigma\left(|E|\right) = \sigma_o + (\sigma_{max} - \sigma_o)\exp[-A \cdot \exp[-B \cdot E]] \qquad (2)$$

where σ_o is the non-electroporated tissue conductivity and σ_{max} is the maximum conductivity for thoroughly permeabilized cells, *A* and *B* are coefficients for the displacement and growth rate of the curve, respectively. Here we assume $\sigma_o = 0.1$ S/m but this value can be scaled by a *factor* to match any other non-electroporated tissue conductivity or material as determined by a pre-treatment pulse. We examined the effect of the ratio between the maximum conductivity post-IRE and baseline conductivity pre-IRE (*Z*) in the resulting electric current using the 50-μs pulse parameters (A = 3.05271; B = 0.00233) reported by Neal et. al [14].

The current density was integrated over the surface of the ground electrode to determine the total current delivered. A regression analysis on the resulting current was performed to determine the effect of the parameters investigated and their

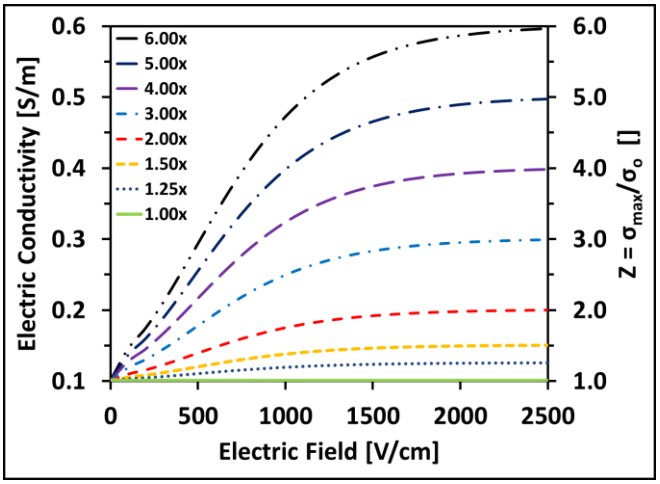

Fig 1: Asymmetrical Gompertz function showing the tissue electric conductivity as a function of electric field.

interactions using the *NonlinearModelFit* function in Wolfram Mathematica 8.0. Current data from the numerical simulations were fit to a mathematical expression that accounted for all possible parameter interactions:

$$\begin{aligned} I = factor \cdot [&aW + bX + cY + dZ + e(W - \overline{W})(X - \overline{X}) + \\ &f(W - \overline{W})(Y - \overline{Y}) + g(W - \overline{W})(Z - \overline{Z}) + \\ &h(X - \overline{X})(Y - \overline{Y}) + i(X - \overline{X})(Z - \overline{Z}) + \\ &j(Y - \overline{Y})(Z - \overline{Z}) + k(W - \overline{W})(X - \overline{X})(Y - \overline{Y}) + \\ &l(X - \overline{X})(Y - \overline{Y})(Z - \overline{Z}) + m(W - \overline{W})(Y - \overline{Y})(Z - \overline{Z}) + \\ &n(W - \overline{W})(X - \overline{X})(Z - \overline{Z}) + \\ &o(W - \overline{W})(X - \overline{X})(Y - \overline{Y})(Z - \overline{Z}) + p] \end{aligned} \qquad (3)$$

where *I* is the current in amps, *W* is the voltage-to-distance ratio [V/cm], *X* is the edge-to-edge distance [cm], *Y* is the exposure length [cm], and *Z* is the unitless ratio σ_{max}/σ_o. The $\overline{W}$, $\overline{X}$, $\overline{Y}$, and $\overline{Z}$ are means for each of their corresponding parameters (Table 1) and the coefficients (*a, b, c, …, n, o, p*) were determined from the regression analysis (Table 2).

Table 1: Electrode configuration and relevant electroporation-based treatment values used in study.

	PARAMETER VALUES	MEAN
W [V/cm]	500, 1000, 1500, 2000, 2500, 3000	1750
X [cm]	0.5, 1.0, 1.5, 2.0, 2.5	1.5
Y [cm]	0.5, 1.0, 1.5, 2.0, 2.5, 3.0	1.75
Z []	1.0, 1.25, 1.5, 2.0, 3.0, 4.0, 5.0, 6.0	2.96875

III. Results

We provide a method to determine electric conductivity change following EBTs using current measurements and the electrode configuration. The best-fit statistical model between the *W*, *X*, *Y*, and *Z* parameters resulted in Eqn. 3 with the coefficients in Table 2 ($R^2 = 0.999646$). Every coefficient and their interactions had statistical significant effects on the resulting current ($P < 0.0001^*$). With this equation one can predict the current for any combination of

the W, Y, X, Z parameters studied within their ranges (500 V/cm ≤ W ≤ 3000 V/cm, 0.5 cm ≤ X ≤ 2.5 cm, 0.5 cm ≤ Y ≤ 3.0 cm, and 1.0 ≤ Z ≤ 6.0). Additionally, by using the linear results (Z = 1), the baseline tissue conductivity can be extrapolated for any blunt-tip electrode configuration by delivering and measuring the current of a non-electroporating pre-treatment pulse. This technique could also be used to determine the conductivity of other materials.

Table 2: Coefficients (P < 0.0001*) from the Least Square analysis using the *NonlinearModelFit* function in Mathematica.

	ESTIMATE		ESTIMATE
a →	0.00820	i →	2.18763
b →	7.18533	j →	1.73269
c →	5.80997	k →	0.00201
d →	3.73939	l →	0.92272
e →	0.00459	m →	0.00129
f →	0.00390	n →	0.00152
g →	0.00271	o →	0.00067
h →	3.05537	p →	-33.92640

Fig. 2 shows a representative case in which the effect of the W and Z are studied for electroporation-based therapies with 2.0 cm electrodes separated by 1.5 cm. The 3D plot corroborates the quality of the model which shows every data point from the numerical simulation (green spheres) being intersected by the best-fit statistical model. This 3D plot also shows that when Z is kept constant within the ranges studied, the current increases linearly with the voltage-to-distance ratio (W). Similarly, the current increases linearly with Z when the voltage-to-distance ratio is constant. However, for all the other scenarios there is a non-linear response in the current that becomes more drastic with simultaneous increases in W and Z.

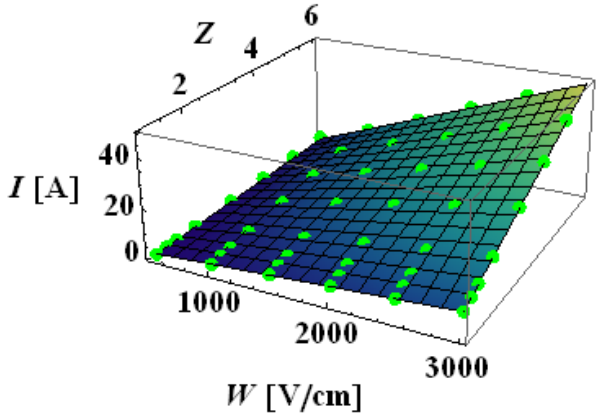

Fig 2: Representative 3D plot of current [A] as a function of Z (σ_{max}/σ_o) and voltage-to-distance ratio (W) for a separation distance of 1.5 cm and an electrode exposure length of 2.0 cm as used by Ben-David et al. [15].

In order to fully understand the predictive capability of the statistical model, we provide two cases in which the current

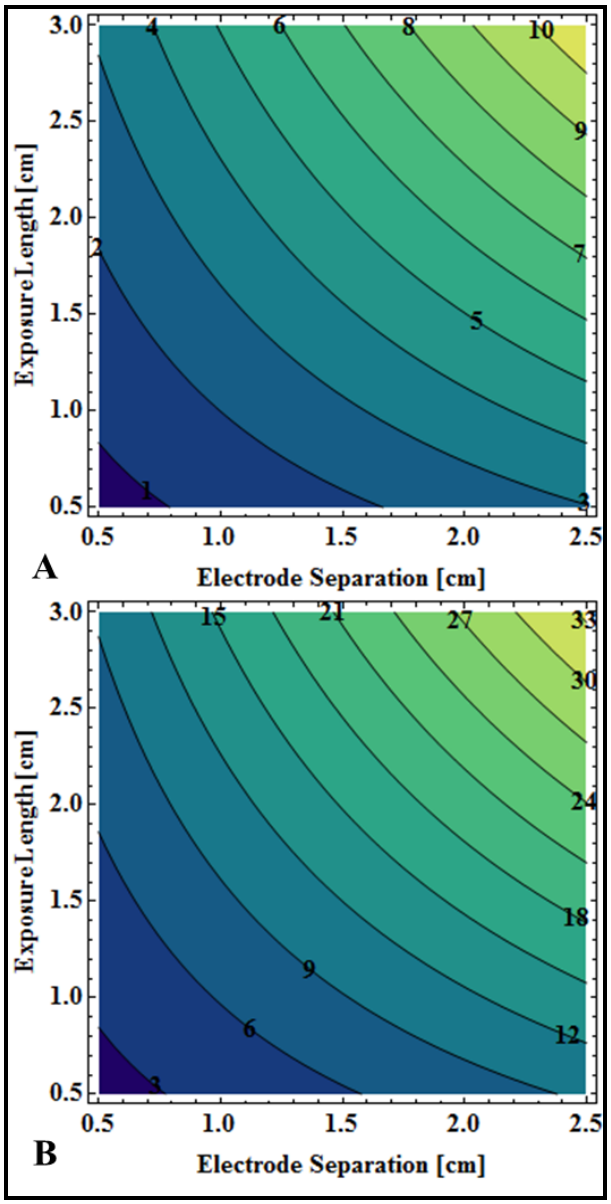

Fig 3: Representative contour plot of current [A] as a function of electrode exposure and separation distance using 1500 V/cm for A) Z = 1 and B) Z = 4.

is presented as a function of the exposure length and electrode separation. Fig. 3 (Panel A) shows the linear case (Z = 1) in which the current can be scaled to predict any other combination of pulse parameters as long as the pulses do not achieve electroporation. For example, one can deliver a non-electroporating pulse (~50 V/cm) and measure current. The current can then be scaled to match one of the W values investigated in this study. By using Eqn. 3 and solving for the *factor*, the baseline electric conductivity of the tissue can be determined and used for treatment planning. Fig. 3 (Panel B) is the case in which the maximum electric conductivity was 0.4 S/m (Z = 4) after electroporation. The trends are similar to the ones described in Fig. 2 in that if exposure length is constant, the current increases with increasing electrode separation and vice versa. However, even though the conductivity within the treated region increases by a

factor of 4, the current increases non-linearly only by a factor of 3. This can be seen by comparing the contours in Fig. 3 (Panel A) with those in Fig. 3 (Panel B) which consistently show that the curves are increased by a factor of 3.

IV. DISCUSSION

This study provides several important considerations when determining treatment parameters for electroporation-based therapies. First, the baseline conductivity of the tissue must be determined before the therapy in order to determine safe and effective pulse protocols. We present a statistical model that uses an asymmetrical Gompertz function to describe the response of porcine renal tissue to electroporation pulses. This model can be used to determine baseline conductivity of tissue based on any combination of electrode exposure length, separation distance, and non-electroporating electric pulses. In addition, the model can be scaled to the baseline conductivity and used to determine the maximum electric conductivity after the electroporation-based treatment. By determining the ratio of conductivities pre- and post-treatment, it is possible to predict the shape of the electric field distribution and thus the treatment volume based on electrical measurements. An advantage of this statistical model is that it is easy to use and no additional electronics or numerical simulations are needed to determine the electric conductivities. The method can also be adapted for other electrode geometries (sharp electrodes, bipolar probes), electrode diameter, and other tissues/tumors once their response to different electric fields has been fully characterized. Future work will incorporate the temperature dependent electric conductivity and will characterize the three-dimensional treatment shape based on the pre- and post-treatment electric conductivity ratio, electrode exposure, separation distance, and voltage-to-distance ratio.

ACKNOWLEDGMENT

The authors thank R.E Neal II and M.B. Sano for their help in the analysis of the data.

REFERENCES

[1] L.M. Mir, M. Belehradek, C. Domenge, S. Orlowski, B. Poddevin, J. Belehradek, Jr., G. Schwaab, B. Luboinski, and C. Paoletti, "Electrochemotherapy, a new antitumor treatment: first clinical trial," *C R Acad Sci III,* 313, 613-8, 1991.

[2] A.I. Daud, R.C. DeConti, S. Andrews, P. Urbas, A.I. Riker, V.K. Sondak, P.N. Munster, D.M. Sullivan, K.E. Ugen, J.L. Messina, and R. Heller, "Phase I Trial of Interleukin-12 Plasmid Electroporation in Patients With Metastatic Melanoma," *Journal of Clinical Oncology,* 26, 5896-5903, Dec. 2008.

[3] R.V. Davalos, L.M. Mir, and B. Rubinsky, "Tissue ablation with irreversible electroporation," *Ann Biomed Eng,* 33, 223-31, Feb. 2005.

[4] R.V. Davalos, D.M. Otten, L.M. Mir, and B. Rubinsky, "Electrical impedance tomography for imaging tissue electroporation," *IEEE Transactions on Biomedical Engineering,* 51, 761-767, 2004.

[5] L. Appelbaum, E. Ben-David, J. Sosna, Y. Nissenbaum, and S.N. Goldberg, "US Findings after Irreversible Electroporation Ablation: Radiologic-Pathologic Correlation," *Radiology,* 262, 117-125, Jan. 2012.

[6] B. Al-Sakere, F. Andre, C. Bernat, E. Connault, P. Opolon, R.V. Davalos, B. Rubinsky, and L.M. Mir, "Tumor ablation with irreversible electroporation," *PLoS ONE,* 2, e1135, 2007.

[7] K.R. Thomson, W. Cheung, S.J. Ellis, D. Federman, H. Kavnoudias, D. Loader-Oliver, S. Roberts, P. Evans, C. Ball, and A. Haydon, "Investigation of the safety of irreversible electroporation in humans," *J Vasc Interv Radiol,* 22, 611-21, May 2011.

[8] R.E. Neal II, J. Rossmeisl, P.A. Garcia, O. Lanz, N. Henao- Guerrero, and R.V. Davalos, "A Case Report on the Successful Treatment of a Large Soft-Tissue Sarcoma with Irreversible Electroporation," *J Clin Oncol,* 29, 1-6, 2011.

[9] P.A. Garcia, T. Pancotto, J.H. Rossmeisl, N. Henao-Guerrero, N.R. Gustafson, G.B. Daniel, J.L. Robertson, T.L. Ellis, and R.V. Davalos, "Non-thermal irreversible electroporation (N-TIRE) and adjuvant fractionated radiotherapeutic multimodal therapy for intracranial malignant glioma in a canine patient," *Technol Cancer Res Treat,* 10, 73-83, 2011.

[10] J.F. Edd and R.V. Davalos, "Mathematical modeling of irreversible electroporation for treatment planning," *Technol Cancer Res Treat,* 6, 275-286, 2007.

[11] D. Sel, D. Cukjati, D. Batiuskaite, T. Slivnik, L.M. Mir, and D. Miklavcic, "Sequential finite element model of tissue electropermeabilization," *IEEE Trans Biomed Eng,* 52, 816-27, May 2005.

[12] S. Corovic, M. Pavlin, and D. Miklavcic, "Analytical and numerical quantification and comparison of the local electric field in the tissue for different electrode configurations," *Biomed Eng Online,* 6, 2007.

[13] D. Cukjati, D. Batiuskaite, F. Andre, D. Miklavcic, and L.M. Mir, "Real time electroporation control for accurate and safe in vivo non-viral gene therapy," *Bioelectrochemistry,* 70, 501-7, May 2007.

[14] R.E. Neal II, P.A. Garcia, J.L. Robertson, and R.V. Davalos, "Experimental Characterization and Numerical Modeling of Tissue Electrical Conductivity during Pulsed Electric Fields for Irreversible Electroporation Treatment Planning," *IEEE Trans Biomed Eng,* 59, 1076-1085, 2012.

[15] E. Ben-David, L. Appelbaum, J. Sosna, I. Nissenbaum, and S.N. Goldberg, "Characterization of Irreversible Electroporation Ablation in In Vivo Porcine Liver," *Am J Roentgenol,* 198, W62-W68, Jan. 2012.